Original Article

MOLECULAR METABOLISM

Heterogeneity in the perirenal region of humans suggests presence of dormant brown adipose tissue that contains brown fat precursor cells

Naja Z. Jespersen [1,2,3,12], Amir Feizi [4,12], Eline S. Andersen [1], Sarah Heywood [1], Helle B. Hattel [1], Søren Daugaard [5], Lone Peijs [1,11], Per Bagi [6], Bo Feldt-Rasmussen [7], Heidi S. Schultz [8], Ninna S. Hansen [3,9], Rikke Krogh-Madsen [1], Bente K. Pedersen [1,2], Natasa Petrovic [10], Søren Nielsen [1,13], Camilla Scheele [1,11,*,13]

ABSTRACT

Objective: Increasing the amounts of functionally competent brown adipose tissue (BAT) in adult humans has the potential to restore dysfunctional metabolism and counteract obesity. In this study, we aimed to characterize the human perirenal fat depot, and we hypothesized that there would be regional, within-depot differences in the adipose signature depending on local sympathetic activity.

Methods: We characterized fat specimens from four different perirenal regions of adult kidney donors, through a combination of qPCR mapping, immunohistochemical staining, RNA-sequencing, and pre-adipocyte isolation. Candidate gene signatures, separated by adipocyte morphology, were recapitulated in a murine model of unilocular brown fat induced by thermoneutrality and high fat diet.

Results: We identified widespread amounts of dormant brown adipose tissue throughout the perirenal depot, which was contrasted by multilocular BAT, primarily found near the adrenal gland. Dormant BAT was characterized by a unilocular morphology and a distinct gene expression profile, which partly overlapped with that of subcutaneous white adipose tissue (WAT). Brown fat precursor cells, which differentiated into functional brown adipocytes were present in the entire perirenal fat depot, regardless of state. We identified SPARC as a candidate adipokine contributing to a dormant BAT state, and CLSTN3 as a novel marker for multilocular BAT.

Conclusions: We propose that perirenal adipose tissue in adult humans consists mainly of dormant BAT and provide a data set for future research on factors which can reactivate dormant BAT into active BAT, a potential strategy for combatting obesity and metabolic disease.

Keywords Perirenal adipose tissue; Brown fat precursor cells; Human brown fat; Sympathetic activation; Dormant brown fat

1. INTRODUCTION

Brown adipose tissue (BAT) provides non-shivering thermogenesis through mitochondrial uncoupling via the BAT specific protein, uncoupling protein 1 (UCP1) [1]. This is an energy consuming process, thus providing a rationale for targeting human BAT as part of an anti-obesity strategy. In accordance, the amount of active human BAT has been found to negatively correlate with body mass index (BMI) [2], whereas BAT activation or recruitment increases metabolic rate [3] and insulin sensitivity [4–7].

An age-dependent shift in BAT morphology was described in early autopsy-histology studies of human BAT, demonstrating that a more white-like phenotype gradually occurred with increasing age, represented by increased lipid accumulation [8,9]. More recent studies utilizing PET/CT-FDG-scans as a read-out have supported this idea, and it has been suggested that the amount of active BAT is greatly reduced after the age of 40 [2,10,11]. The decline in BAT activity with age was further emphasized by a large retrospective study of PET/CT-FDG scanned patients [12]. However, these studies should be interpreted with caution as detecting the maximal active BAT capacity using the PET/CT-FDG technique seems to require an individualized cooling protocol [13], which was not applied in the above-mentioned pioneer studies. Interestingly, in a study of retroperitoneal adipose tissue (including perirenal fat), the BAT specific protein Mitochondrial brown

[1]The Centre of Inflammation and Metabolism and Centre for Physical Activity Research Rigshospitalet, University Hospital of Copenhagen, 2100, Denmark [2]Faculty of Health and Medical Sciences, University of Copenhagen, Copenhagen, Denmark [3]Danish PhD School of Molecular Metabolism, Odense, Denmark [4]Novo Nordisk Research Center Oxford, Denmark [5]Department of Pathology, Rigshospitalet, Denmark [6]Department of Urology, Rigshospitalet, Denmark [7]Department of Nephrology, Rigshospitalet, Denmark [8]Novo Nordisk A/S, Måløv, Denmark [9]Department of Endocrinology, Diabetes and Metabolism, Rigshospitalet, Denmark [10]Department of Molecular Biosciences, The Wenner-Gren Institute, The Arrhenius Laboratories F3, Stockholm University, 106 91, Stockholm, Sweden [11]Novo Nordisk Foundation Center for Basic Metabolic Research, Faculty of Health and Medical Sciences, University of Copenhagen, Denmark

[12] Shared first authorship.

[13] Shared last authorship.

*Corresponding author. Blegdamsvej 3B, 2200, Copenhagen, Denmark. E-mail: cs@sund.ku.dk (C. Scheele).

Received January 18, 2019 • Revision received March 2, 2019 • Accepted March 11, 2019 • Available online 15 March 2019

https://doi.org/10.1016/j.molmet.2019.03.005

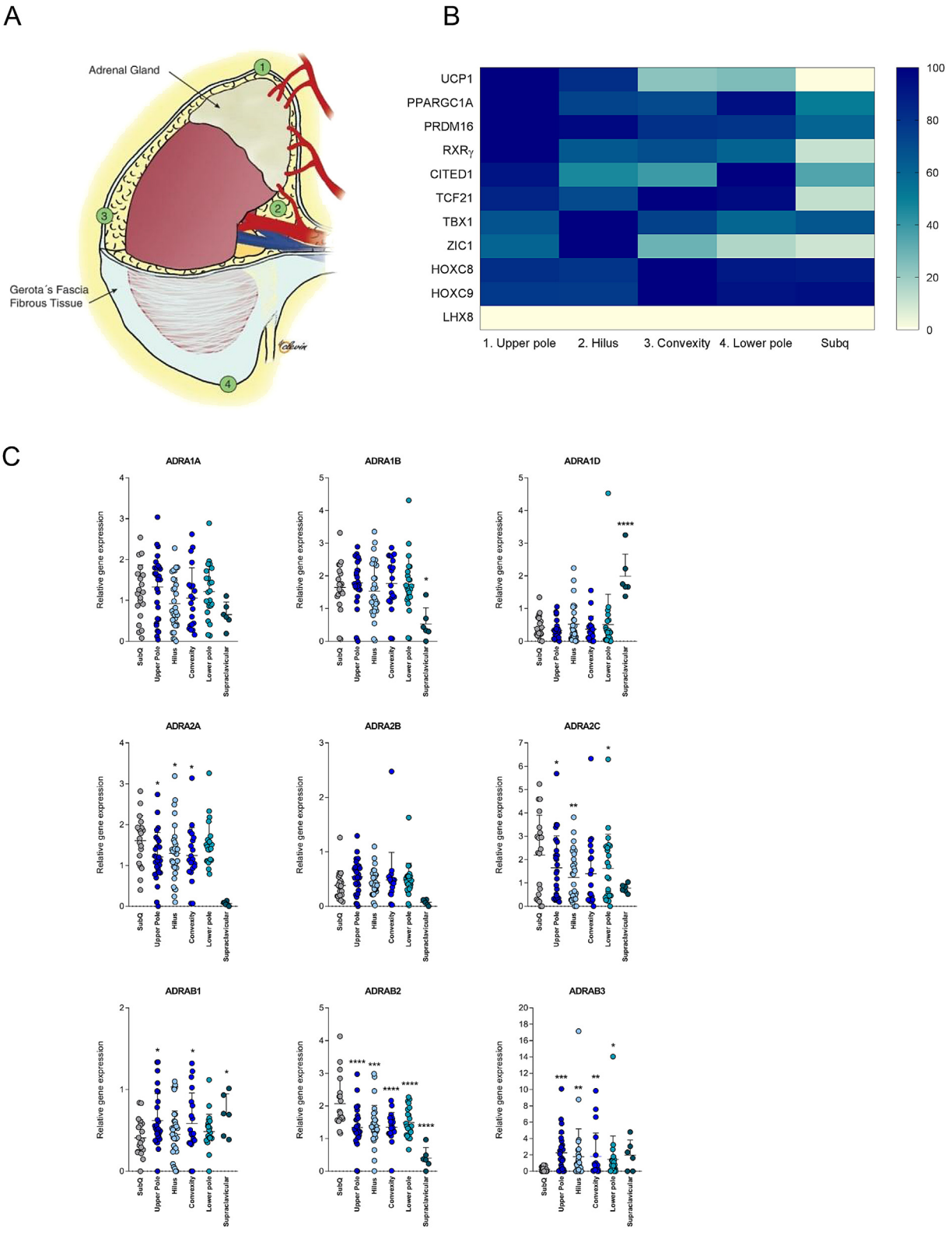

Figure 1: qPCR profiling of perirenal adipose tissue. (A) The human kidney with numbers annotating the regions for the obtained surgical biopsies: 1 = upper kidney pole, 2 = hilus, 3 = convexity and 4 = lower kidney pole. A subcutaneous fat biopsy was obtained from the incision site at the abdomen. **(B)** Heatmap illustrating relative gene expression levels of marker genes measured by using qPCR. Regions are sorted based on UCP1 expression. **(C)** Gene expression profiling of adrenergic receptors by using qPCR. Individual values are shown and data are presented as mean with error bars representing standard deviation (SD). * = $P < 0.05$, ** = $P < 0.01$, *** = $P < 0.001$, **** = $P < 0.0001$.

fat uncoupling protein 1 (UCP1) was present in around 50% of middle-aged adult humans and was inversely correlated with outdoor temperature [14]. These findings suggest that BAT is still present in older individuals and that a dynamic environmental adaptation of BAT activity occurs in humans.

Here, we further investigated the perirenal adipose depot, in which UCP1 expression previously has been detected in adults [14–19]. Perirenal fat surrounds the kidney as well as the adrenal gland, which secretes epinephrine and norepinephrine (NE) in response to sympathetic activation, and the kidney in general is heavily sympathetically innervated [20]. Compared to WAT, which is composed of unilocular adipocytes, cold-responsive BAT is multilocular with many smaller lipid droplets in each adipocyte. We hypothesized that multilocular BAT would accumulate close to the adrenal gland and in the hilus region where sympathetic nerve endings enter the depot, and we aimed to characterize the molecular differences between this fat compared to perirenal fat more distant from these sources of norepinephrine.

2. METHODS AND EXPERIMENTAL PROCEDURES

2.1. Subjects

20 Subjects (11 men and 9 women) were included prior to scheduled kidney donation through the outpatient clinic of the Nephrological Department, Rigshospitalet after providing informed written consent. Participants were included throughout the period of June 2014 and March 2015. All subjects were examined in accordance with the custom kidney donor screening programme and were thus healthy. Anthropometrics and clinical measurements were obtained from the patient files or during the patient interview prior to participation. No additional examinations were performed, and there were no additional exclusion criteria if subjects were considered eligible for donation. The Scientific-Ethics Committee of the Capital region of Copenhagen approved the study protocol, journal number H-1-2013-144, and the study was performed in accordance with the Helsinki declaration.

2.2. Biopsies

Adipose tissue biopsies were collected during nephrectomy. Samples were collected from 3 to 7 areas of the perirenal fat layer surrounding the kidney. The number and specific location of the biopsies depended on the explicit fat distribution in each subject. Furthermore, a subcutaneous fat biopsy was collected from the incision site at the abdomen of all subjects. Samples were divided into 3 parts; the part for mRNA analyses was immediately snap frozen in liquid nitrogen and stored at −80° until analyses were performed, while samples for immunohistochemistry were placed in formalin until further processing. Perirenal fat samples were obtained from both inside and outside Gerota's fascia (Figure 1A) at the level of the 2 kidney poles and the convexity, whereas the hilus as such is located inside the fascia. However, since no systematic differences between samples from inside and outside the fascia were observed, samples were pooled into the 4 anatomical regions described in the result section. Three tissue samples were excluded from the analyses due to unspecific registration of their localization. Six supraclavicular samples from a previously published article [21] were included as reference material in the analyses of adrenergic receptor expression.

2.3. RNA isolation and quantitative real-time PCR (qPCR)

Total RNA isolation from adipose tissue biopsies or cultured adipocytes was performed using TRizol reagent according to the manufacturer's protocol. RNA was dissolved in nuclease-free water and quantified using a Nanodrop ND 1000 (Saveen Biotech). Total RNA (0.25 μg) was reverse-transcribed using the High Capacity cDNA Reverse Transcription Kit (Applied Biosystems). cDNA samples were loaded in triplicate and qPCR was performed using Real Time quantitative PCR, using the ViiA^{tm} 7 platform (Applied Biosystems). Relative quantification was conducted by either SYBRgreen fluorescent dye (Applied Biosystems) or TaqMan Gene Expression Assays (Applied Biosystems). All procedures were performed according to the manufacturer's protocol. Target mRNA expression was calculated based on the standard curve method and was normalized to the reference gene PPIA. Median CT values and efficiency of the qPCR assays for adipose type marker genes and adrenergic receptors are annotated in Tables S1 and S2. Primer sequences are found in Table S3.

2.4. Isolation, culture and differentiation of human adipogenic progenitor cells

Primary cell cultures were established and cultured as previously described [21]. Adipogenic progenitor cells were isolated from the stromal vascular fraction of the biopsies on the day they were obtained. Biopsies were collected in DMEM/F12 (Gibco) with 1% penicillin/streptomycin (PS; life technologies) and tubes were kept on ice during transport from the operating room to the cell-lab. Biopsies were digested in a buffer containing 10 mg collagenase II (C6885-1G, Sigma) and 100 mg BSA (A8806-5G, Sigma) in 10 ml DMEM/F12 for 20–30 min at 37 °C while gently shaken. Following digestion, the suspension was filtered through a cell strainer (70 μm size) and cells were left to settle for 5 min before the layer below the floating, mature adipocytes was filtered through a thin filter (30 micron). The cell suspension was centrifuged for 7 min at 800 g, and the cell pellet was washed with DMEM/F12 and then centrifuged again before being resuspended in DMEM/F12, 1% PS, 10% fetal bovine serum (FBS) (Life technologies) and seeded in a 25 cm^2 culture flask. Media was changed the day following isolation and then every second day until cells were 80% confluent; at this point, cultures were split into a 10 cm dish (passage 0).

Cells were expanded by splitting 1:3. At passage 1, cells were seeded for gene expression experiments in proliferation media consisting of DMEM/F12, 10% FBS, 1% PS and 1 nM Fibroblast growth factor-acidic (FGF-1) (ImmunoTools). Cells were grown at 37 °C in an atmosphere of 5% CO2 and the medium was changed every second day. Adipocyte differentiation was induced two days after preadipocyte cultures were 100% confluent by addition of a differentiation cocktail consisting of DMEM/F12 containing 1% PS, 0.1 μM dexamethasone (Sigma–Aldrich), 100 nM insulin (Actrapid, Novo Nordisk or Humulin, Eli Lilly), 200 nM rosiglitazone (Sigma–Aldrich), 540 μM isobutylmethylxanthine (Sigma–Aldrich), 2 nM T3 (Sigma–Aldrich) and 10 μg/ml transferrin (Sigma–Aldrich). After three days of differentiation, isobutylmethylxanthine was removed from the cell culture media, and after an additional three days rosiglitazone was removed from the media for the remaining 6 days of differentiation. On the 12th day of differentiation the media was changed to DMEM/F12, 1% PS for 2 h before stimulation with 10 μM norepinephrine (Sigma Aldrich, A9512 L- (−)-Norepinephrine (+)-bitartrate salt monohydrate diluted in sterile H2O) or sterile H2O. After 4 h of stimulation, cells were harvested using TRizol (Invitrogen) and stored on −80 °C until PCR analyses were performed.

The degree of cell differentiation was evaluated based on a combination of visual evaluation of the amount of accumulated lipid droplets (% of culture) on the day of stimulation and FABP4 mRNA expression (Figure S2). For seven of the cultures, no visual estimation had been registered; thus, only FABP4 expression was used for the estimation in these cultures.

On the final day of differentiation, cultures were stimulated with either 10 μM of NE or vehicle treatment before being harvested for gene expression analyses.

Adipogenic progenitor cells were isolated from all participants, but only cultures from 18 of the subjects were included in the study, total cell strain N = 86, (13 subcutaneous and 73 perirenal). Cultures from 2 subjects were excluded due to infection, and one culture was excluded based on complete lack of differentiation. The availability of the cell cultures for other research groups is dependent on specific permission from the Danish Data Protection Agency and on the researcher's adherence to the specifications of this permission.

2.5. Flow cytometry

Flow cytometry was performed on cells from passage three to evaluate adipogenic potential of the isolated cells. The cells were proliferated according to standard protocol in DMEM/F12 medium supplemented with 10% FBS, 1% PS, and 1 nmol/L fibroblast growth factor in 5% CO2, 37 °C environment until they reached 80% confluence. Cells were harvested using TrypLE (Gibco; Life Technologies) followed by a wash in buffer (PBS containing 2% FBS and 0.01% NaN3) and were afterwards resuspended in staining buffer (PBS containing 2% FBS, 1% Human Serum [catalog #1001291552; Sigma] and 0.01% NaN3). Anti-human CD45-APC, CD31-FITC, CD90- PerCP.Cy5.5, and CD166-PE (BD Pharmingen), antibodies were added to the cells and flow cytometry was applied for quantification using a FACS Fortessa (BD Bioscience). For compensation, single stain was used with one drop of negative control beads and anti-mouse IgG beads (BD Biosciences). Data analysis was performed using Kaluza software, version 1.2 (Beckman Coulter).

2.6. Cell imaging

When pre-adipocytes reached a confluence at 80% they were fixated in 4% formaldehyde (15 min) and then permeabilized in 0.5% Triton X-100 (15 min). F-actin was then labeled with ActinGreen™ 488 ReadyProbes® (Thermo Fisher) for 30 min and DAPI (Thermo Fisher) for visualization of the nucleus. Imaging was performed with EVOS FL Cell Imaging System (Thermo Fisher).

2.7. Oxygen consumption analyses

Oxygen consumption was measured using a Seahorse Bioscience XF96 Extracellular Flux Analyzer according to the manufacturer's protocol. Adipocytes were grown until reaching 100% confluency and were then seeded in Seahorse plates at a 1:1 ratio and differentiated as described above. Experiments were performed on day 12 of differentiation on cells in passage three. Oxygen consumption rate was assessed in 20 primary adipocyte cultures, four per region. The sample set was selected based on approximately equal degree of differentiation. The results were extracted from the Seahorse Program Wave 2.2.0. Baseline measurements of OCR were performed for 30 min before NE or saline was added and measurements of the concomitant responses were recorded for 60 min. All other states were induced using the seahorse XF cell mito stress test kit according to the manufactures protocol. After 90 min, leak state was induced by adding Oligomycin, which inhibits the ATP synthase. Leak state measurements were performed for 20 min, then the ionophore (carbonyl cyanide-4-(trifluoromethoxy) phenylhydrazone) (FCCP), which collapses the proton gradient across the mitochondrial inner membrane resulting in a completely uncoupled state. After an additional 20 min Antimycin A and Rotenone were added to inhibit complexes III and I respectively, resulting in only non-mitochondrial respiration.

For data analyses OCR was corrected for non-mitochondrial respiration as assessed by the Seahorse XF cell mitochondrial stress test kit. To adjust for a slight decrease in OCR during the first 90 min OCR changes were calculated as the difference between the NE treated wells and the saline treated wells and data analyses were performed. Wells were excluded from the data analyses if OCR were +/−20% of the mean in that series of replicate values. In total 17 wells were excluded based on this.

2.8. Immunohistochemistry

Immunohistochemical analyses of UCP1, RXRγ, and PRDM16 were performed at the Pathological Department, Rigshospitalet. The tissue samples were placed in 10% neutral-buffered formalin and processed routinely. After fixation for about 24 h, the tissue was placed in cassettes and transferred to a Leica Peloris Rapid Tissue Processor (Leica Biosystems GmbH, Nussloch, Germany). The tissue was then paraffin-embedded and sectioned manually and stained with hematoxylin-eosin (HE). The immunohistochemical reactions were performed using a BenchMark ULTRA IHC/ISH Staining Module with Optiview visualization reagents (Ventana Medical Systems Inc., Tucson, Arizona, USA). Immunostainings were performed using: UCP1: Rabbit-polyclonal UCP1-antibody (Abcam), dilution 1:500, pretreatment pH 9 (32 min) + protease3 (4 min), RXRγ: Rabbit-polyclonal RXRγ-antibody (Abcam), dilution 1:2000, pretreatment pH 9 (32 min), PRDM16: Rabbit-polyclonal antibody (Abcam), dilution, 1:500, pretreatment pH 6 (32 min). Sections were evaluated as follows: multilocular appearance in the HE-staining and UCP1 positive (MBAT), HE unilocular and UCP1 positive (UBAT+) or both HE unilocular and UCP1 negative (UBAT-). Samples were considered as MBAT if UCP1 positive multilocular cells were present in the section, irrespective of their amount. No attempt to quantify the amount of the respective cell types in each section was performed. PRDM16 (nuclear) stains were scored as either positive or negative, i.e. if there were any positive (nuclear reaction) in any of the cells present. No attempt was made to quantitate these results. RXRγ stainings (nuclear) were scored as positive or with only few positive cells. For UCP1 staining, a hibernoma tissue section was included as positive and negative control. Samples were evaluated by the author SD.

2.9. Protein expression

Perirenal and subcutaneous protein expression was assessed by western blotting. Primary antibodies were used at the following concentrations: UCP1 (Abcam ab155117; 1:1000), tyrosine hydroxylase (Abcam ab112; 1:200) and OXPHOS (Abcam ab110413; 1:1000). Primary antibodies were detected with either anti-rabbit or anti-mouse horseradish peroxidase-linked IgG (Dako) at a concentration of 1:5000 and imaged using Supersignal West Femto (Pierce). Data are expressed relative to total protein expression using stain free UV imaging (Biorad) and normalized to a pooled perirenal sample included on all gels. Gels were quantified using Image Lab version 5.2.1 software (Biorad).

2.10. Transcriptional profiling of human multilocular and unilocular BAT and subcutaneous WAT

A subset of the surgical biopsies described above was selected for RNA sequencing. Three groups (two perirenal and one subcutaneous) of n = 4 samples were selected. The samples for the two perirenal groups had either multilocular morphology or unilocular morphology and were both positive for UCP1 protein. To increase the likelihood that the unilocular sample for RNA analysis did not contain multilocular adipocytes, we selected unilocular samples with low UCP1

expression. The subcutaneous samples were from the same individual as the unilocular samples. The samples for RNA sequencing were anonymized. RNA was isolated using Trizol according to the manufacturer's recommendations and quality control was performed using Nanodrop and Bioanalyzer. RNA sequencing (PE 100) was performed on a HiSeq 4000 platform after Truseq cDNA library construction on poly-A tail filtered RNA (BGI, Copenhagen, Denmark). The transcriptome data from 12 tissues samples were processed and analyzed by RNA-seq analysis pipeline from CLC Genomics workbench 11 (https://www.qiagenbioinformatics.com/). The human genome reference hg38 were used for the mapping and annotation with the default setting. We chose the *total counts* options for calculating the expression values. For the differential expression analysis, we used all groups pairs comparison including the FDR <0.01 as cut off. The expression values are normalized using TMM method (trimmed mean of M values) [22] to calculate the effective libraries sizes followed by z-score calculation. The Gene Ontology enrichment analysis on the differentially expressed (DE) genes was performed using the clusterProfiler R package [23]. We used 0.05 q-value cut off for the term enrichment of the DE genes.

2.11. Mouse model for dormant BAT

All experiments were approved by the Animal Ethics Committee of the North Stockholm region. Metabolic data including e.g. body weight, body composition, food intake, glucose tolerance, and insulin tolerance from the mouse study have been published previously [24]. Briefly, 12-week-old male mice were single-caged at thermoneutrality (30 °C) in a 12:12-h light–dark cycle regime for at least 25 weeks. Mice were randomized in two groups given either chow (R70, Lactamin) (n = 5) or high fat diet (45% calories from fat, Research Diets D12451) (n = 5), ad libitum. Multilocular BAT (interscapular) was obtained by housing mice at room temperature, representing mild cold stimulation for a mouse [25], and on chow diet. Unilocular BAT (interscapular) and unilocular WAT (inguinal) was obtained by housing mice at thermoneutrality and on high-fat diet [24,26]. Mice were sacrificed by CO_2 anesthesia. Interscapular BAT and inguinal white adipose tissue was dissected, snap-frozen in liquid nitrogen, and stored in −80 °C until further analysis. Total RNA was extracted using TRI reagent and cDNA synthesis and quantitative real-time PCR was performed as previously described [24]. The primer sequences are presented in supplementary material.

2.12. Knockdown of SPARC

Adipogenic progenitor cells derived from the deep neck supraclavicular depot of adult humans (n = 2 non-immortalized cell strains) [21] were differentiated as described above (n = 3 independent experiments for each cell culture). At day three of differentiation, SPARC was knocked down using ON-TARGETplus SMARTPOOL siRNA, consisting of a pool of four different oligos targeting different sites of the mRNA transcript (Dharamcon). An ON-TARGETplus Non-targeting Pool was used as control. For transfection, 20 nM siRNA was used with RNAimax lipofectamine (Thermofisher Scientific), according to the manufacturer's protocol.

2.13. Statistical analyses

Statistical analyses were performed using SAS 9.4 statistical software. Data are presented as means and standard deviation (SD) unless stated otherwise. Analyses were performed using repeated measures mixed models ANOVA with Tukey correction unless stated otherwise, and a P-value below 0.05 was considered significant (Littell et al., 2006). Logarithmic transformation was applied in all analyses when appropriate to attain normal distribution. Correlations between UCP1 expression and other genes, were analyzed using ordinary least squares (OLS) regression analyses with manual backwards elimination of independent variables. Tables and figures were designed using GraphPad Prism 7.

3. RESULTS

We recruited 20 kidney donors, aged 37–68 years, to investigate the status of adult perirenal fat, a depot consisting of BAT during infancy. The subjects were healthy and included both men (n = 11) and women (n = 9). The physiological characteristics of the subjects are summarized in Table 1.

3.1. BAT marker profiling suggests presence of dormant BAT

We characterized adipose tissue surrounding four perirenal regions including the upper kidney pole, the hilus, the convexity, and the lower kidney pole in a cohort of healthy adults, while subcutaneous fat from the surgical incision site on the abdomen was included for comparison (Figure 1A). Selected BAT markers, previously identified in murine studies and used for characterization of human supraclavicular fat [21,28–30], were mapped using qPCR (Figure 1B). For some subjects, multiple samples were collected from each region. In these cases, the sample with the highest level of UCP1 was chosen for analysis of all markers, thus including the upper kidney pole (n = 18), the hilus (n = 20), the convexity (n = 16), and the lower kidney pole (n = 17). We found the highest UCP1 expression in the region closest to the adrenal gland, where markers involved in the brown fat transcription program, i.e. PGC-1α [31] and PRDM16 [32] also accumulated, while the region most distant to the adrenal gland displayed the lowest UCP1 expression (Figure 1B). Notably, LHX8, a previously annotated marker for human supraclavicular BAT [21], was completely lacking in the perirenal BAT. A full marker gene expression comparison including all samples for all subjects, in total 121 tissue samples, was also performed, confirming the gene expression pattern observed in the heatmap (Figure S1A). This analysis demonstrated that UCP1 was expressed to a higher degree in all perirenal regions compared to subcutaneous fat (Figure S1A) and that UCP1 mRNA levels at the upper kidney pole were higher than at the lower pole and the convexity (Figure S1A). Furthermore, the BAT activity genes, PPARGC1A [31] and CITED1 [21,29], were higher expressed in the perirenal upper pole only when comparing the perirenal regions to subcutaneous fat (Figure S1A). In contrast, the human perirenal BAT marker RXRγ displayed higher expression in all the perirenal regions compared to subcutaneous fat (Figure S1A). Whereas human perirenal and supraclavicular BAT have several markers in common, some markers previously described as human BAT selective (LHX8 and TBX1) or white fat selective (HOXC8 and HOXC9) (Figure S1A and Figure S2) [21,30] were not differentially regulated between subcutaneous and perirenal fat, and might thus mainly reflect anatomical location. This is however not excluding that these genes have a role in adipocyte phenotype as HOXC8 has been reported to negatively control browning of white fat [33].

Table 1 — Subject characteristics.

Sex (N)	Age (years)	BMI (kg/m^2)
Men (11)	55 (38–68)	26 (24–37)
Women (9)	54 (37–67)	25 (16–28)

Data are median and range. Abbreviations: BMI; Body mass index.

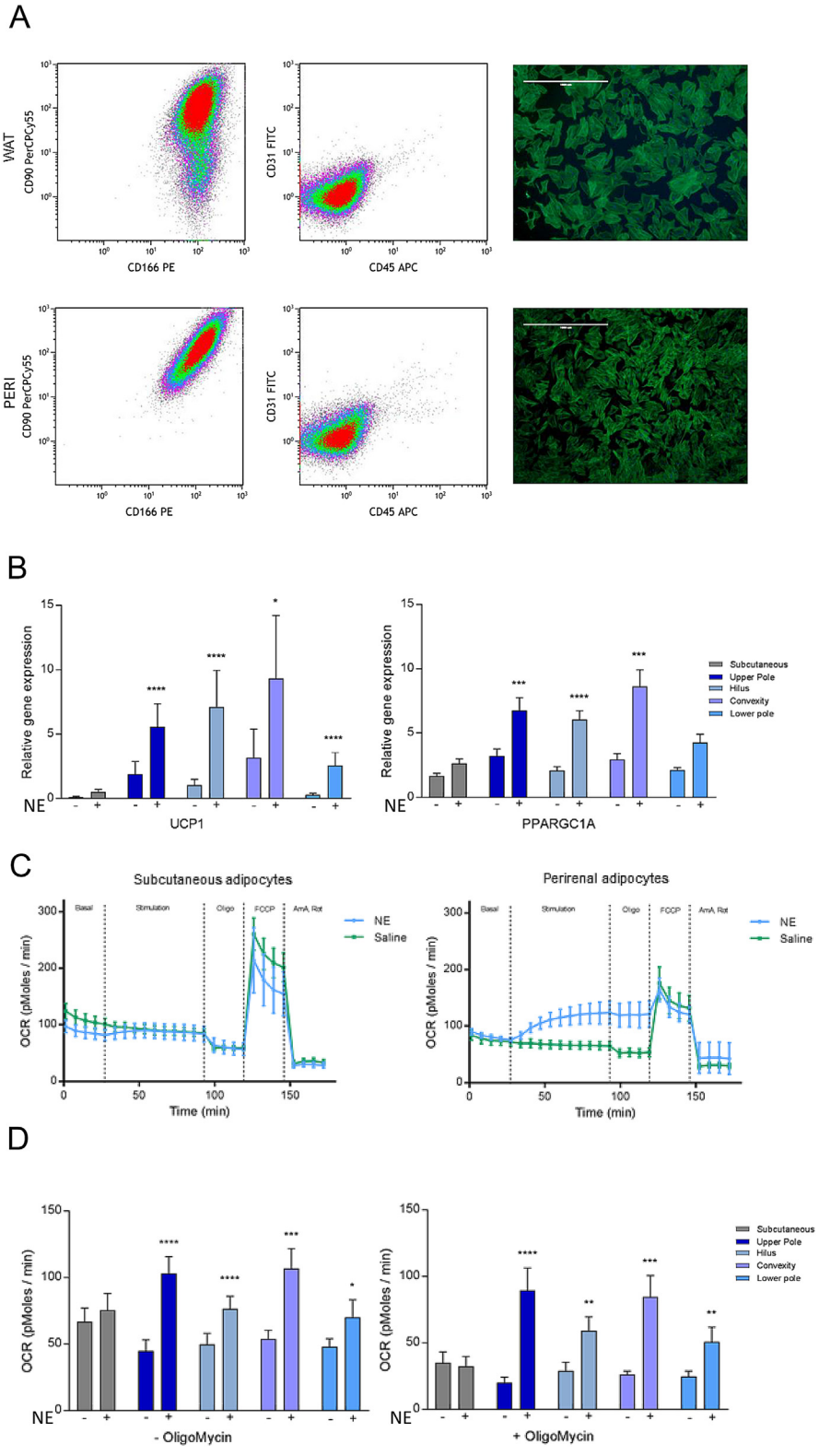

Figure 2: Characterization of adipogenic progenitors derived from perirenal fat of adults. Adipogenic progenitors were isolated from the four regions of the perirenal depot, as depicted in Figure 1, and from the subcutaneous depot. **(A)** Representative density plots for adipogenic characterization by using Flow cytometry, and pre-adipocytes at 4X magnification, stained with fluorescently-labeled phalloidin and DAPI (scale bar = 1000 μm). **(B)** Gene expression response to 4 h of NE treatment of in vitro differentiated adipocytes from perirenal and subcutaneous regions. Data are presented as mean +/− standard error of the mean (SEM), * = $P < 0.05$, *** = $P < 0.001$ **** = 0.0001. **(C)** Representative traces of NE-induced uncoupled respiration of subcutaneous and perirenal adipocytes **(D)** Comparison of basal and NE-induced respiration in subcutaneous and perirenal adipocytes with and without the ATP synthase blocker oligomycin. Data are mean +/−SEM. * = $p < 0.05$, ** = $P < 0.01$, **** = $p < 0.0001$.

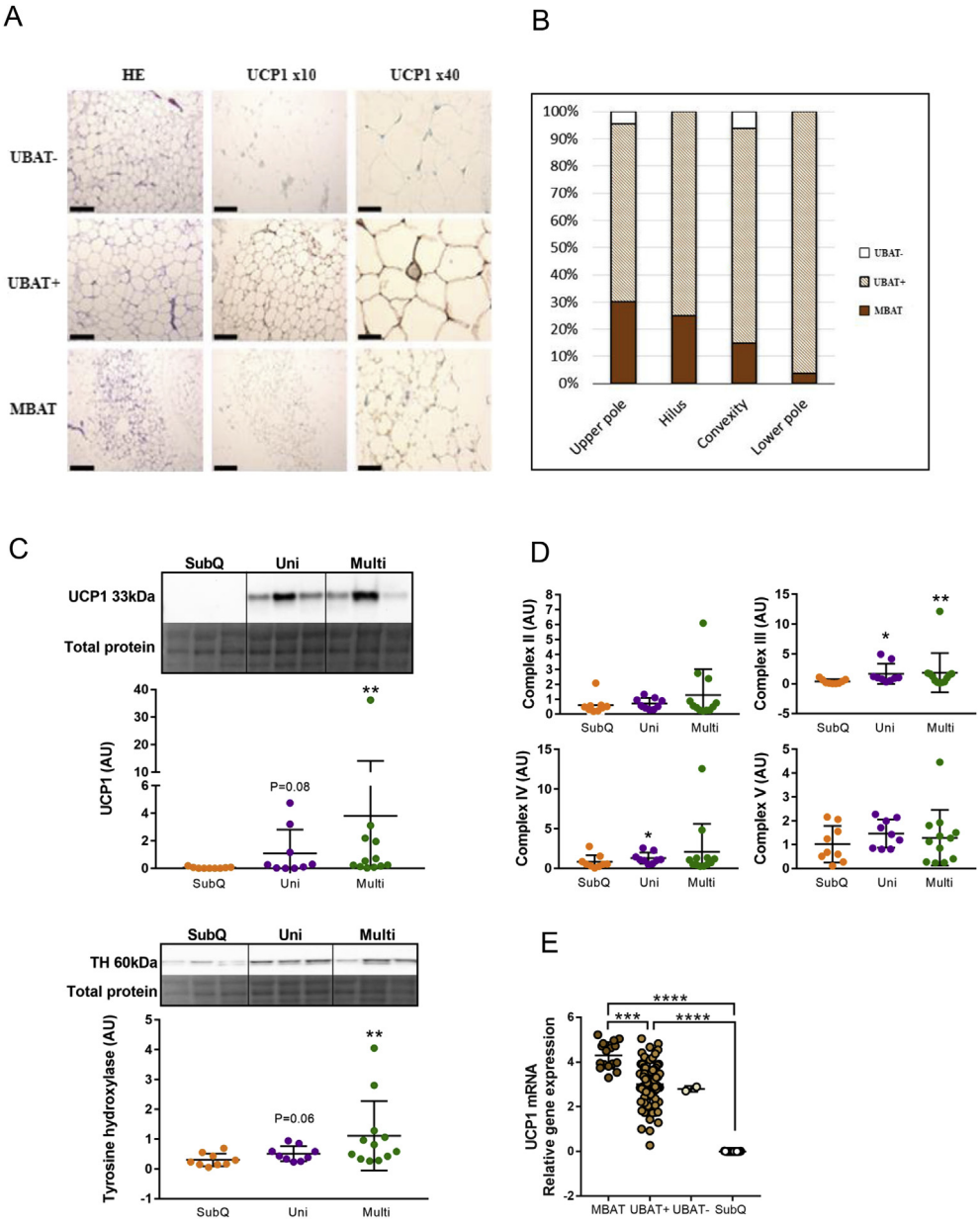

Figure 3: The brown fat phenotypes in perirenal tissue of adult humans. (A) Morphological and immunohistochemical evaluation of human perirenal fat. Representative H&E staining and UCP1 staining of areas with multilocular UCP1 positive brown adipose tissue (MBAT) unilocular BAT (UBAT+), and unilocular UCP1 negative BAT (UBAT-). Bar scale = 240 μm in left and middle panel and 60 μm in right panel. **(B)** Percentage distribution of MBAT, UBAT+ and UBAT-samples in the different perirenal regions. **(C)** UCP1 and Tyrosine hydroxylase (TH) western blotting. A section the total protein assessment is shown and was used for normalization. **(D)** mitochondrial OXPHOS western blotting. Complex I was too weak to quantify (Figure S3D). **(E)** UCP1 mRNA expression in groups based on histology data. Individual values are shown and data are mean +/− SD. When the error bar reached below 0, it was clipped by the GraphPad software and in these cases, only the upper error bar is shown and indicates the variation; *P < 0.05, **P < 0.01, ***P < 0.001.

We next performed a qPCR mapping of the gene expression of nine different α- and β-adrenergic receptors in the four perirenal regions, including subcutaneous WAT and supraclavicular BAT as references. The α-receptors ADRA1B and ADRA1D had a differential regulation pattern in supraclavicular adipose tissue compared to the perirenal depots, indicating a difference between these depots. Importantly, we found that the β3-adrenergic receptor (ADRB3), which is responsible for the main BAT activation pathway in rodents [1], was substantially higher in *all* perirenal regions compared to subcutaneous adipose tissue and was not different from supraclavicular BAT (Figure 1C). The ADRB3 expression in the perirenal adipose tissue from the upper pole was most significantly higher than in the subcutaneous depot. The individual variation in all depots was high, possibly reflecting the exposure of adrenergic activity in these samples. ADRB1 and ADRB2 were equally expressed in all perirenal regions (Figure 1C). These findings suggest a variable, but sustained NE-sensitivity in the entire perirenal fat depot.

3.2. Brown fat precursor cells are present in all perirenal regions

To further characterize the molecular differences between the perirenal adipose regions, we isolated adipogenic progenitor cells from the above-described adipose regions using our established protocol [21].

Table 2 — Genes correlated to UCP1 in unilocular and multilocular tissue samples.

Genes	morphology	P-value	β-coefficient
UCP1 vs. RXRγ	Uni	<0.0001	1.52
UCP1 vs. PPARGC1A	Uni	<0.05	0.36
UCP1 vs. HOXC8	Uni	<0.05	−0.47
UCP1 vs. HOXC8	multi	<0.05	−1.37
UCP1 vs. RXRγ	multi	<0.05	1.29

Analyses were performed using multivariate OLS regression analyses between log10 [UCP1] applying manual backwards elimination of independent variables. Overall model P-value < 0.0001, adjusted R2 multi = 0.37, adjusted R2 uni = 0.42.

In a subset (n = 4 from each region), we found the cells to be negative for CD31 (endothelial marker) and CD45 (hematopoietic stem cell marker) while staining positive for CD90 and CD166, demonstrating high adipogenic potential, which was equal between regions (Figure 2A) [34]. This was further supported by gene expression analysis of differentiation markers (Figure S2). In total, we isolated cell cultures from n = 18 subjects and from each of the four perirenal regions as well as from subcutaneous WAT at the surgical incision site. UCP1 was up-regulated in response to 4 h of NE treatment of in vitro differentiated cells derived from all perirenal fat regions but not in the cells isolated from the subcutaneous depot (Figure 2B), and a similar response was observed for PPARGC1A [31,35] (Figure 2B). None of the other investigated markers were regulated in response to NE or differentially expressed between perirenal and subcutaneous adipocytes (Figure S2B). Consistently, we found that in vitro differentiated preadipocytes derived from perirenal fat responded to NE by inducing uncoupled respiration, which was in contrast to the lacking response observed in adipocytes originating from subcutaneous adipose tissue (Figure 2C,D). This response was regardless of region and, thus, regardless of a dormant state at the tissue level as shown in Figure 1. Taken together, we conclude that brown fat progenitors, which can differentiate into functional brown adipocytes, are present in all regions of perirenal fat assessed in the current study.

3.3. UCP1-positive unilocular BAT dominates perirenal fat in adult humans

We next determined the morphology and UCP1 protein expression in the above-described perirenal regions. By using immunohistochemistry, we defined three types of adipocytes: multilocular, UCP1 positive (MBAT); unilocular, UCP1-positive (UBAT+), and unilocular, UCP1-negative (UBAT-) (Figure 3A). Importantly, unilocular UCP1-positive adipocytes have previously been observed in human perirenal fat [18]. In total, 20% of all samples were classified as MBAT, and MBAT was detected in 60% of the participants. UBAT+ was observed in nearly all perirenal samples of the dataset, while only 1.8% of the samples were completely negative for UCP1 (UBAT-) (Figure 3B). Additional staining examples and controls are provided (Figure S3A, B). MBAT was observed at highest frequency by the upper kidney pole (30%), followed by the hilus (25%), the convexity (15.7%) and the lower pole (3.6%) (Figure 3B), while UBAT+ was found in all subjects and in all perirenal regions. Immunohistochemical stainings of RXRγ [18] were positive in all perirenal samples, whereas 88% of perirenal fat samples were positive for PRDM16 [36] (Figure S3C). No selection towards MBAT positive areas was observed for either RXRγ or PRDM16 positivity. Western blot analysis confirmed that both multilocular and unilocular samples were positive for UCP1 protein (Figure 3C). Tyrosine hydroxylase was higher in the multilocular samples, suggesting higher sympathetic activation (Figure 3C), which is in line with previous morphological observations [37]. However, similarly to the UCP1 protein expression, there was no difference in OXPHOS protein levels between unilocular and multilocular samples (Figure 3D). We next divided our UCP1 mRNA data based on multilocular and unilocular annotation and observed that a high UCP1 mRNA expression seemed to coincide with a multilocular morphology (Figure 3E). UCP1 mRNA levels correlated positively with PPARGC1a and RXRγ and negatively with HOXC8 [21,33,38] in both multilocular and unilocular samples (Table 2). There were no significant correlations between UCP1 tissue expression and donor age, BMI or mean or minimum outdoor temperature in the week prior to surgery (data not shown). Taken together, these results suggest that a large pool of dormant BAT, distinct from subcutaneous fat, is widely present in the entire perirenal fat depot, even in subjects around 60 years of age.

3.4. The gene signature of human dormant BAT

To investigate the molecular signature of the dormant BAT state, we performed RNA sequencing on a subset of perirenal multilocular and unilocular samples. Subcutaneous samples were included from the same individuals as the unilocular samples were retrieved from. Multilocular samples were selected from biopsies were a multilocular phenotype had been observed and were UCP1 mRNA expression was high. Unilocular samples with low UCP1 mRNA levels were selected and paired subcutaneous samples were included (n = 4 for each adipose tissue type). A principal component analysis (PCA) of the transcriptome readouts, including all identified genes in all samples, demonstrated a separation into three subpopulations. These subpopulations were, with the exception of one subject, defined by the origin of the samples (i.e. subcutaneous, unilocular or multilocular) (Figure 4A). Next, we used neighbor joining algorithms to cluster samples based on statistically significant differentially expressed genes (FDR < 0.01). This resulted in fat tissue type-dependent clustering of the multilocular, unilocular and subcutaneous groups, suggesting that these groups were defined by unique gene expression signatures (Figure 4B and Figure S4A). Strikingly, several mitochondrial genes were higher expressed in multilocular compared to both unilocular and subcutaneous samples, including the mitochondrially transcribed: MT-CO1, MT-CYB, MT-ATP6, MT-ND4, MT-ND1, MT-CO2, MT-CO3. Moreover, genes transcribed from the nucleus with mitochondria-associated gene products were higher, including the BAT-specific UCP1 and its transcriptional coactivator PPARGC1A. In concordance with previous studies [39,40], various forms of a key protein in mitochondrial respiration, Creatine kinase, were also higher in the multilocular samples. Taken together, these observations suggest a higher metabolic activity in the multilocular fat compared to the subcutaneous and the unilocular fat (Figure 4B). A volcano plot, based on $-\log_{10}$ p-values versus $\log_2$ fold change, revealed CLSTN3 as the most significantly regulated gene between the two conditions, higher in biopsies with multilocular BAT (Figure 4C). Another top candidate was KCNK3 (encoding Potassium channel subfamily K member 3), which was previously reported to be higher expressed in immortalized human brown adipocytes compared to white adipocytes, and to be important for thermogenic function [41], supporting the idea of the multilocular adipose samples representing a more active BAT phenotype compared to the unilocular adipose samples. A Venn diagram demonstrated that most of the differentially expressed genes ($\log_2$ fold change cut off of 2 and FDR <0.01) were specific for each analyzed adipose type. (Figure 4D). Gene ontology analysis (Figure 4E and S4B) of differentially expressed genes further emphasized a major difference in cellular respiration between unilocular and multilocular

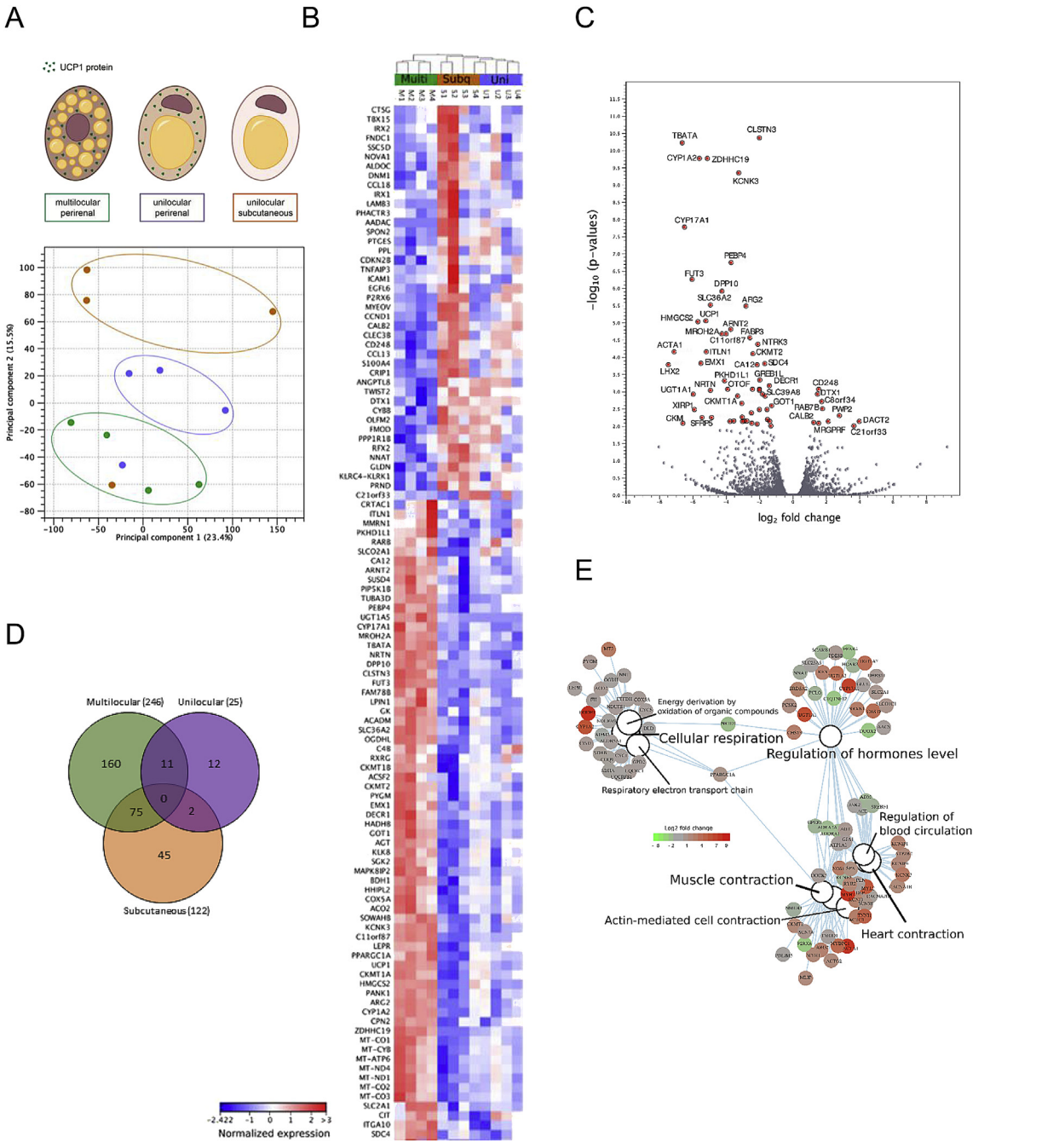

Figure 4: RNA sequencing of multilocular and unilocular perirenal fat and subcutaneous fat. (A) Principal component analysis (PCA) plot based on all detected genes in RNA sequencing of multilocular perirenal, unilocular perirenal and unilocular subcutaneous adipose tissue samples **(B)** Heatmap of the most differentially expressed genes (FDR < 0.01) between the three tissue types. **(C)** Volcano plot ranking genes after -log10 p-value (y-axis) and log2 fold change (x-axis). Differentially expressed genes (p-value < 0.01) are shown with red dots. **(D)** Venn diagram demonstrating the number of specific/overlaps of differentially expressed genes (FDR < 0.01) for each of the three tissue types. **(E)** Category netplot generated by the clusterProfiler R package [23]. This network plot shows the relationships between the genes associated with the top most significant GO terms (q-value < 0.05) and their corresponding significant fold changes (FDR < 0.01) from multilocular perirenal vs. unilocular perirenal comparison. The log2 foldchange color code is next to the network and the size of the GO terms reflects the q-values of the terms, with the more significant terms being larger.

samples. We furthermore observed a shift in genes regulating hormonal levels, and since adipose tissue has an established role in hormonal regulation, our findings raise the possibility of differential roles in hormonal regulation between active and dormant BAT. Finally, there was a difference in genes involved in muscle contraction between the two fat phenotypes. This was somewhat surprising to us, but might be related to the increased mitochondrial activity combined with the established developmental link between brown adipose tissue and skeletal muscle [36,38].

3.5. Reduction in SPARC increase adrenergic response in brown adipocytes

To identify candidate genes involved in the function or regulation of dormant BAT, we screened for genes with largest fold change

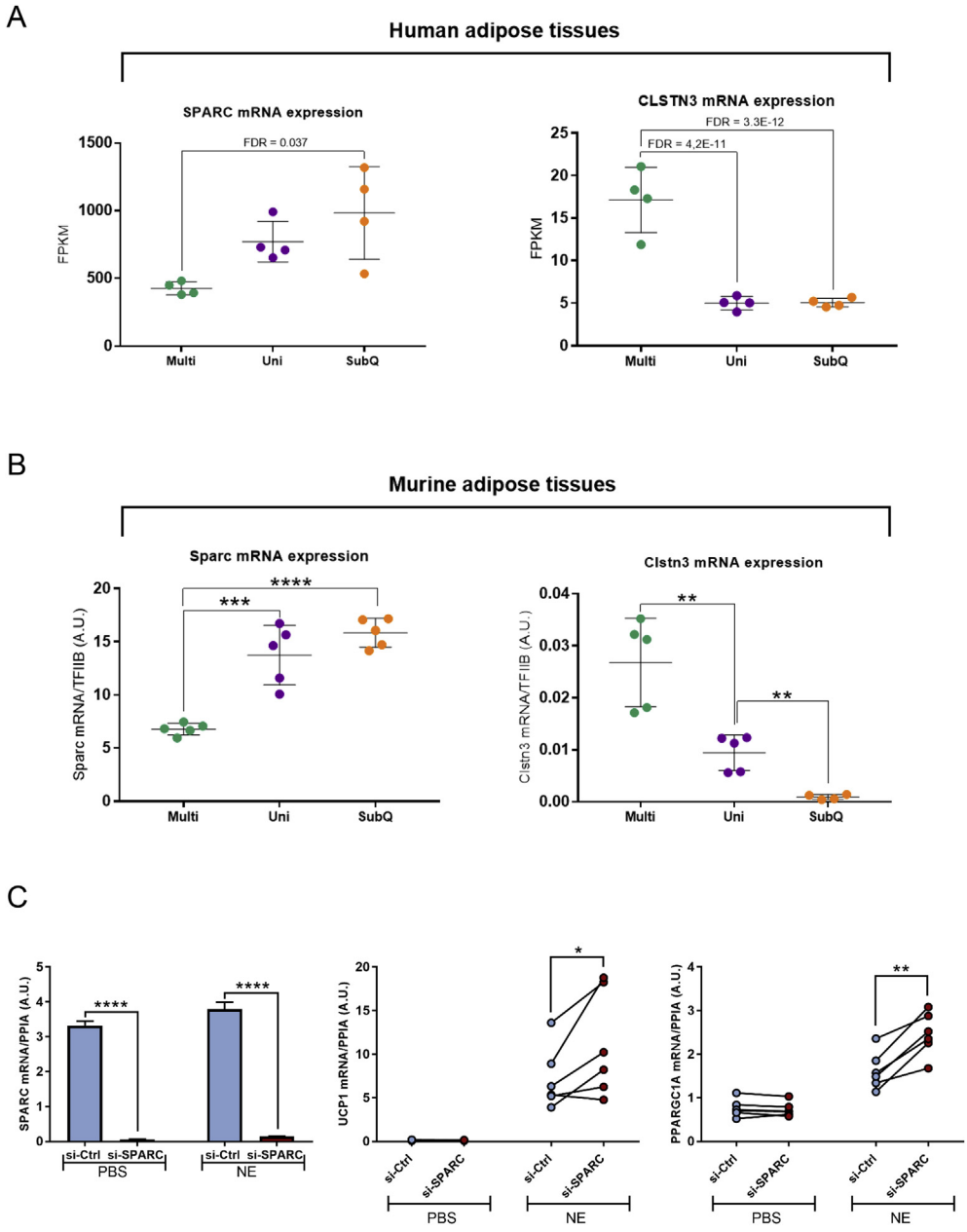

Figure 5: Validation of candidate dormant BAT genes. (A) SPARC and CLSTN3 in multilocular perirenal fat (multi); unilocular perirenal fat (uni) and subcutaneous fat (subq). Data are adjusted gene counts (FPKM) and adjusted p-values (FDR) from the RNA sequencing analysis are annotated in the figure. Error bars represent SD. **(B)** Sparc and Clstn3 in a mouse model of dormant BAT. Gene expression analysis was performed by using qPCR. Data are mean +/− SD. Unpaired t-tests between multi IBAT and uni IBAT: *P < 0.05, **P < 0.01, ***P < 0.001. Paired t-tests between uni IBAT and uni IWAT $^{\$}$P < 0.05, $^{\$\$}$P < 0.01, $^{\$\$\$}$P < 0.001. **(C)** Brown pre-adipocytes were transfected with siRNA targeting SPARC (si-SPARC) or with a non-targeting siRNA control (si-Ctrl) and stimulated with NE upon differentiation. Gene expression was measured using qPCR. Data are mean +/− SEM (SPARC) or individual values (UCP1 and PPARGC1A) *P < 0.05, **P < 0.01, ***P < 0.001.

differences between the two most distinct groups, subcutaneous WAT and multilocular BAT. To take the gene expression levels and data dispersion between groups into account, we sorted after standard deviation. Among the top three genes, we identified SPARC (Adj. p-value: 0.037), a secreted protein which previously was shown to influence and interact with extracellular matrix to regulate cell growth and differentiation [42]. We plotted the RPKM values for SPARC and observed a lower expression in multilocular compared to subcutaneous samples with unilocular samples appearing in between the two extreme groups. In contrast, CLSTN3, the top candidate gene from the Volcano plot, displayed a low expression in both unilocular and subcutaneous compared to multilocular (Figure 5A).

To further validate the concept of dormant BAT and our candidate genes from adult humans, we utilized a previously established mouse model in which unilocularity was induced in classical BAT by long-term thermoneutrality and high-fat diet [25,26]. Convincingly, we found that the gene expression pattern of Sparc and Clstn3 in the mouse model was consistent with the pattern observed in the human sample set, supporting the existence of dormant BAT in the perirenal fat of adult humans and the validity of these candidate genes (Figure 5B). Interestingly,

SPARC has been shown to have an opposing expression pattern to UCP1 in hibernating arctic ground squirrels [43]. This could suggest a suppressive role of SPARC in relation to BAT activation.
To address a potential suppressing effect of SPARC on multilocular BAT adipogenesis and activity, we performed siRNA-mediated knockdown of SPARC in non-immortalized human deep neck brown adipocytes [21,44] at day three of differentiation. Following differentiation, we stimulated mature adipocytes with NE for 4 h prior to harvest and RNA isolation. Knockdown of SPARC was highly efficient both at basal and under NE-stimulated conditions (Figure 5C). Reduced levels of SPARC during differentiation resulted in increased responsiveness to NE in terms of upregulation of UCP1 (Figure 5C) and PGC-1α (Figure 5C). These data support a role of SPARC in promoting a dormant state of BAT.

4. DISCUSSION

We here identify a dormant BAT state in the perirenal adipose and demonstrate that multilocular adipocytes accumulate near sources of local sympathetic activity while unilocular, yet UCP1 positive adipocytes dominates more distant regions. Importantly, brown fat progenitor cells were present regardless of location. Transcriptomic analysis suggested reduced mitochondrial respiration in the unilocular samples compared to the multilocular samples. CLSTN3 was identified as a marker for multilocular BAT. SPARC was higher expressed in unilocular BAT, and knockdown increased norepinephrine responsiveness, suggesting a functional role of SPARC in mediating a dormant BAT state.
Functionally competent BAT has been found less frequently in humans with increasing age as estimated by FDG-PET/CT scans [2,10–12]. However, due to lack of individualized cooling, it remains to be established whether these observations depend on decreased amounts of active BAT, or rather on an increased activation threshold of the sympathetic nervous system.
Our subjects were healthy kidney donors, mainly around 50–60 years of age, and would according to above-mentioned reports, be expected to have low, if any, PET/CT detectable active BAT. This would probably be particularly pronounced in the perirenal depot as a craniocaudal activation pattern of BAT has been observed [45]. Thus, it has been described that the supraclavicular depot can be most easily activated, followed by the mediastinal, the paravertebral and the perirenal depot in that order [45]. Although PET/CT-scans combined with cooling were not applied in the current study, these observations imply that a discrepancy between the frequent reports of the existence of morphological brown adipocytes in perirenal fat and the rarer reports of glucose uptake into this depot is likely to exist. In line with this notion a recent study provided an FDG-PET/CT scan-based atlas, supporting the possibility of high amounts of inactive or "dormant" BAT in anatomically defined fat depots [8,46].
Thus, adult human BAT contains substantial subpopulations of dormant BAT, and our finding that this dormant BAT shows some similarities with WAT is interesting to compare with previous studies in rodents of an inducible thermogenic phenotype within WAT [47,48]. The thermogenic transcription program can be induced in adipocytes residing in WAT via enhancement of PPARγ or PRDM16, and these cells are known as brite [47] or beige [48]. Formation of thermogenic adipocytes in WAT initially occurs through de novo recruitment of preadipocytes [49] which is induced through β3-adrenergic activation of bipotential progenitors [50], proposing sympathetic activity as a major inducer of this phenotype. Another study confirmed that cold stimulation increased formation of brite adipocytes but also reported that a subsequent warm adaptation temporarily reversed this thermogenic phenotype into a white adipocyte-like state [51]. Interestingly, a second cold challenge mediated a switch back to a thermogenic phenotype, suggesting that the white adipocyte-like state during warm conditions reflected a dormant BAT state [51]. This temperature-dependent flexibility was further illustrated by a correlation between outdoor temperature and the amount of BAT in the perirenal depot of adult humans [14].
The common dormant BAT phenotype of human perirenal adipocytes and murine inguinal adipocytes, give reason to revisit the discussion on whether BAT of adult humans is similar to murine beige/brite adipose tissue. Indeed, previous studies have shown that human BAT display some overlapping gene expression signatures with murine beige/brite fat [21,30]. Morphologically, beige/brite adipose tissue is similar to the heterogenous blend of multilocular and unilocular adipocytes comprising BAT of adult humans. However, an important distinction is that the heterogeneity of murine beige adipose is a result of *increased* sympathetic activity, whereas the heterogeneity of BAT in adult humans, as suggested by our current data, is present without exposing subjects to chronic cold challenges. This suggests a higher capacity of browning of adult human BAT compared to murine beige/brite adipose tissue. Indeed, previous cooling studies in adult humans have demonstrated increased BAT activity and improved metabolic function in vivo [52]. Furthermore, the capacity of browning in adult humans is exemplified during Pheochromocytoma, a norepinephrine-producing tumor on the adrenal gland [37,53]. Here, browning mainly occurs in the the areas were BAT has been morphologically mapped during childhood (with the exception of the interscapular adipose depot, which is no longer present in adults) [8], identifying these regions as major targets for in vivo browning in humans [53].
The accumulation of multilocular BAT near the adrenal gland in our healthy subjects is consistent with PET-CT reports describing the most pronounced FDG signal close to the upper kidney pole [54,55]. A possible explanation for this observation is that sympathetic nerves highly innervate, and supply NE to the endothelium of blood vessels, which enter the kidney via the hilus and the adrenal gland directly as illustrated in Figure 1A. This idea is supported by anatomical studies investigating the distribution of sympathetic fibers in relationship to renal vascularization, demonstrating that 90.5% of all nerves were found within 2.0 mm from the lumen of the renal arteries [56]. Interestingly, the ability of the perirenal adipocyte progenitors to differentiate into functional brown adipocytes appears to be maintained irrespective of the amount of active multilocular BAT in adult humans, as illustrated by the lack of correlation between UCP1 levels in the tissue and the UCP1 levels in the in vitro differentiated preadipocytes from the corresponding perirenal regions. This underscores a sustained flexibility of human perirenal fat which, similarly to rodent BAT, appears to be able to shift between a lipid storing dormant brown adipose type and a thermogenic, metabolically active brown adipose type, dependent on sympathetic activity.

5. CONCLUSION

We here demonstrate that most of the perirenal fat in adult humans consist of dormant BAT, while small amounts of adipocytes with a multilocular morphology and gene expression signature of active BAT, are present near regions where local sources of sympathetic activity is expected to be high. Our data suggest that BAT in adult humans is more abundant than previously anticipated and our comparative transcriptomic analysis provides a resource for identification of novel regulators of BAT activation. Targeting such regulators might prove an efficient strategy to reactivate BAT and revitalize metabolism in adult humans.

AUTHOR CONTRIBUTIONS

CS and SN supervised the study. CS, SN, NZJ, NP, BKP, RKM: hypothesis generation, conceptual design, data analysis, and manuscript

preparation. NZJ, AF, ESA, SH, HBH, SN, NP, SD, LP, PB, BFR, HSS, NSH: conducting experiments and data analysis. All authors edited and approved the final manuscript.

DISCLOSURE OF LIMITED AVAILABILITY OF BIOLOGICAL MATERIAL AND SEQUENCING DATA

We hereby disclose that the availability of biological material including the human cell cultures, as well as accessibility to raw counts from the sequencing data is dependent on specific permission from the Danish Data Protection Agency and on the researcher's adherence to the specifications of such a permission. Please contact the corresponding author if any requests.

DISCLOSURE OF COMPETING FINANCIAL INTERESTS

Heidi Schultz is an employee and shareholder of Novo Nordisk A/S.

ACKNOWLEDGEMENTS

We thank the study participants; the staff at the Departments of Nephrology and Urology, Rigshospitalet in particular Søren Schwartz Sørensen and Lene Kjær Olsen; Noemi G. James and Maria M. Scheel and Pernille Frederiksen for technical assistance; the Department of Biostatistics at University of Copenhagen for statistical advice. The Centre for Physical Activity Research (CFAS) is supported by a grant from TrygFonden. During the study period the Centre for Inflammation and Metabolism (CIM) was supported by a grant from the Danish National Research Foundation (DNRF55). Novo Nordisk Foundation Center for Basic Metabolic Research is an independent Research Center, based at the University of Copenhagen, Denmark and partially funded by an unconditional donation from the Novo Nordisk Foundation (www.cbmr.ku.dk, http://www.cbmr.ku.dk/) (Grant number NNF18CC0034900.) The study was further supported by research grants from the Lundbeck Foundation, the Danish Diabetes Academy supported by the Novo Nordisk Foundation, The University of Copenhagen, the Research foundation of Rigshospitalet, Carl and Ellen Hertz Foundation, The Foundation of 1870, Oda and Hans Svenningsens Foundation, The Foundation of the Family Hede Nielsen. CIM/CFAS is a member of DD2 - the Danish Center for Strategic Research in Type 2 Diabetes (the Danish Council for Strategic Research, grant no. 09-067009 and 09-075724).

CONFLICT OF INTEREST

None declared.

APPENDIX A. SUPPLEMENTARY DATA

Supplementary data to this article can be found online at https://doi.org/10.1016/j.molmet.2019.03.005.

REFERENCES

[1] Cannon, B., Nedergaard, J., 2004. Brown adipose tissue: function and physiological significance. Physiological Reviews 84(1):277–359. https://doi.org/10.1152/physrev.00015.2003.

[2] Saito, M., Okamatsu-Ogura, Y., Matsushita, M., Watanabe, K., Yoneshiro, T., Nio-Kobayashi, J., et al., 2009. High incidence of metabolically active brown adipose tissue in healthy adult humans: effects of cold exposure and adiposity. Diabetes 58(7):1526–1531. https://doi.org/10.2337/db09-0530.

[3] Cypess, A.M., Weiner, L.S., Roberts-Toler, C., Elía, E.F., Kessler, S.H., Kahn, P.A., et al., 2015. Activation of human brown adipose tissue by a β3-adrenergic receptor agonist. Cell Metabolism 21(1):33–38. https://doi.org/10.1016/j.cmet.2014.12.009.

[4] Hanssen, M.J.W., Hoeks, J., Brans, B., van der Lans, A. a J.J., Schaart, G., van den Driessche, J.J., et al., 2015. Short-term cold acclimation improves insulin sensitivity in patients with type 2 diabetes mellitus. Nature Medicine 21(July): 6–10. https://doi.org/10.1038/nm.3891.

[5] Chondronikola, M., Volpi, E., Borsheim, E., Porter, C., Annamalai, P., Enerback, S., et al., 2014. Brown adipose tissue improves whole-body glucose homeostasis and insulin sensitivity in humans. Diabetes 63(12):4089–4099. https://doi.org/10.2337/db14-0746.

[6] Lee, P., Smith, S., Linderman, J., Courville, A.B., Brychta, R.J., Dieckmann, W., et al., 2014. Temperature-acclimated brown adipose tissue modulates insulin sensitivity in humans. Diabetes 63(11):3686–3698. https://doi.org/10.2337/db14-0513.

[7] Hanssen, M.J.W., Van Der Lans, A.A.J.J., Brans, B., Hoeks, J., Jardon, K.M.C., Schaart, G., et al., 2016. Short-term cold acclimation recruits brown adipose tissue in obese humans. Diabetes. https://doi.org/10.2337/db15-1372.

[8] Heaton, J.M., 1972. The distribution of brown adipose tissue in the human. p. 35–9.

[9] Tanuma, Y., Tamamoto, M., Ito, T., Yokochi, C., 1975. The occurrence of brown adipose tissue in perirenal fat in Japanese. Archivum Histologicum Japonicum Nihon Soshikigaku Kiroku 38(1):43–70.

[10] Yoneshiro, T., Aita, S., Matsushita, M., Okamatsu-Ogura, Y., Kameya, T., Kawai, Y., et al., 2011. Age-related decrease in cold-activated brown adipose tissue and accumulation of body fat in healthy humans. Obesity (Silver Spring, Md.) 19(9):1755–1760. https://doi.org/10.1038/oby.2011.125.

[11] Yoneshiro, Aita, S., Matsushita, M., Kayahara, T., Kameya, T., Kawai, Y., et al., 2013. Recruited brown adipose tissue as an antiobesity agent in humans. Journal of Clinical Investigation 123(8):3404–3408. https://doi.org/10.1172/JCI67803.

[12] Gerngroß, C., Schretter, J., Klingenspor, M., Schwaiger, M., Fromme, T., 2017. Active Brown fat during 18F-FDG PET/CT imaging defines a patient group with characteristic traits and an increased probability of Brown fat redetection. Journal of Nuclear Medicine – Official Publication Society of Nuclear Medicine 58(7):1104–1110. https://doi.org/10.2967/jnumed.116.183988.

[13] van der Lans, A.A.J.J., Wierts, R., Vosselman, M.J., Schrauwen, P., Brans, B., van Marken Lichtenbelt, W.D., 2014. Cold-activated brown adipose tissue in human adults: methodological issues. American Journal of Physiology Regulatory Integrative and Comparative Physiology 307(2):R103–R113. https://doi.org/10.1152/ajpregu.00021.2014.

[14] Betz, M.J., Slawik, M., Lidell, M.E., Osswald, A., Heglind, M., Nilsson, D., et al., 2013. Presence of brown adipocytes in retroperitoneal fat from patients with benign adrenal tumors: relationship with outdoor temperature. Journal of Clinical Endocrinology and Metabolism. https://doi.org/10.1210/jc.2012-3535.

[15] Li, X., Liu, J., Wang, G., Yu, J., Sheng, Y., Wang, C., et al., 2015. Determination of UCP1 expression in subcutaneous and perirenal adipose tissues of patients with hypertension. Endocrine. https://doi.org/10.1007/s12020-015-0572-3.

[16] Van Den Beukel, J.C., Grefhorst, A., Hoogduijn, M.J., Steenbergen, J., Mastroberardino, P.G., Dor, F.J.M.F., et al., 2015. Women have more potential to induce browning of perirenal adipose tissue than men. Obesity 23(8). https://doi.org/10.1002/oby.21166 n/a-n/a.

[17] Nagano, G., Ohno, H., Oki, K., Kobuke, K., Shiwa, T., Yoneda, M., et al., 2015. Activation of classical Brown adipocytes in the adult human perirenal depot is highly correlated with PRDM16–EHMT1 complex expression. PLoS One 10(3): e0122584. https://doi.org/10.1371/journal.pone.0122584.

[18] Svensson, P.A., Lindberg, K., Hoffmann, J.M., Taube, M., Pereira, M.J., Mohsen-Kanson, T., et al., 2014. Characterization of brown adipose tissue in the human perirenal depot. Obesity 22(8):1830–1837. https://doi.org/10.1002/oby.20765.

[19] Vergnes, L., Davies, G.R., Lin, J.Y.J., Yeh, M.W.M., Livhits, M.J.M., Harari, A., et al., 2016. Adipocyte browning and higher mitochondrial function in periadrenal but not SC fat in pheochromocytoma. The Journal of Cinical Endocrinology and Metabolism 101(11):4440–4448. https://doi.org/10.1210/jc.2016-2670.

[20] Goldstein, D.S., Eisenhofer, G., Kopin, I.J., 2003. Sources and significance of plasma levels of catechols and their metabolites in humans. Journal of Pharmacology and Experimental Therapeutics 305(3):800–811. https://doi.org/10.1124/jpet.103.049270.

[21] Jespersen, N.Z., Larsen, T.J., Peijs, L., Daugaard, S., Homøe, P., Loft, A., et al., 2013. A classical brown adipose tissue mrna signature partly overlaps with brite in the supraclavicular region of adult humans. Cell Metabolism 17(5): 798–805. https://doi.org/10.1016/j.cmet.2013.04.011.

[22] Robinson, M.D., Oshlack, A., 2010. A scaling normalization method for differential expression analysis of RNA-seq data. Genome Biology 11(3). https://doi.org/10.1186/gb-2010-11-3-r25.

[23] Yu, G., Wang, L.-G., Han, Y., He, Q.-Y., 2012. clusterProfiler: an R Package for comparing biological themes Among gene clusters. Omics A Journal of Integrative Biology 16(5):284–287.

[24] Abreu-Vieira, G., Fischer, A.W., Mattsson, C., De Jong, J.M.A., Shabalina, I.G., Rydén, M., et al., 2015. Cidea improves the metabolic profile through expansion of adipose tissue. Nature Communications 6(May). https://doi.org/10.1038/ncomms8433.

[25] Sanchez-Gurmaches, J., Tang, Y., Jespersen, N.Z., Wallace, M., Martinez Calejman, C., Gujja, S., et al., 2018. Brown fat AKT2 is a cold-induced kinase that stimulates ChREBP-mediated de novo lipogenesis to optimize fuel storage and thermogenesis. Cell Metabolism 27(1):195–209. https://doi.org/10.1016/j.cmet.2017.10.008.

[26] Fischer, A.W., Shabalina, I.G., Mattsson, C.L., Abreu-Vieira, G., Cannon, B., Nedergaard, J., et al., 2017. UCP1 inhibition in Cidea-overexpressing mice is physiologically counteracted by brown adipose tissue hyperrecruitment. American Journal of Physiology – Endocrinology and Metabolism 312(1): E72–E87. https://doi.org/10.1152/ajpendo.00284.2016.

[28] Lidell, M.E., Betz, M.J., Leinhard, O.D., Heglind, M., Elander, L., Slawik, M., et al., 2013. Evidence for two types of brown adipose tissue in humans. Nature Medicine 19(5):631–634. https://doi.org/10.1038/nm.3017.

[29] Sharp, L.Z., Shinoda, K., Ohno, H., Scheel, D.W., Tomoda, E., Ruiz, L., et al., 2012. Human BAT possesses molecular signatures that resemble beige/brite cells. PLoS One 7(11):e49452. https://doi.org/10.1371/journal.pone.0049452.

[30] Wu, J., Boström, P., Sparks, L.M.M., Ye, L., Choi, J.H.H., Giang, A.-H.H., et al., 2012. Beige adipocytes are a distinct type of thermogenic fat cell in mouse and human. Cell 150(2):366–376. https://doi.org/10.1016/j.cell.2012.05.016.

[31] Puigserver, P., Wu, Z., Park, C.W., Graves, R., Wright, M., Spiegelman, B.M., 1998. A cold-inducible coactivator of nuclear receptors linked to adaptive thermogenesis. Cell 92(6):829–839. https://doi.org/10.1016/S0092-8674(00)81410-5.

[32] Seale, P., Kajimura, S., Yang, W., Chin, S., Rohas, L.M., Uldry, M., et al., 2007. Transcriptional control of Brown fat determination by PRDM16. Cell Metabolism 6(1):38–54. https://doi.org/10.1016/j.cmet.2007.06.001.

[33] Mori, M., Nakagami, H., Rodriguez-Araujo, G., Nimura, K., Kaneda, Y., 2012. Essential role for miR-196a in brown adipogenesis of white fat progenitor cells. PLoS Biology 10(4):e1001314. https://doi.org/10.1371/journal.pbio.1001314.

[34] Schultz, N., Broholm, C., Gillberg, L., Mortensen, B., Jørgensen, S.W., Schultz, H.S., et al., 2014. Impaired leptin gene expression and release in cultured preadipocytes isolated from individuals born with low birth weight. Diabetes 63(1):111–121. https://doi.org/10.2337/db13-0621.

[35] de Jong, J.M.A., Larsson, O., Cannon, B., Nedergaard, J., 2015. A stringent validation of mouse adipose tissue identity markers. American Journal of Physiology Endocrinology and Metabolism 308(12):E1085–E1105. https://doi.org/10.1152/ajpendo.00023.2015.

[36] Seale, P., Bjork, B., Yang, W., Kajimura, S., Chin, S., Kuang, S., et al., 2008. PRDM16 controls a brown fat/skeletal muscle switch. Nature 454(7207):961–967. https://doi.org/10.1038/nature07182.

[37] Frontini, A., Vitali, A., Perugini, J., Murano, I., Romiti, C., Ricquier, D., et al., 2013. White-to-brown transdifferentiation of omental adipocytes in patients affected by pheochromocytoma. Biochimica et Biophysica Acta 1831(5):950–959. https://doi.org/10.1016/j.bbalip.2013.02.005.

[38] Timmons, J.A., Wennmalm, K., Larsson, O., Walden, T.B., Lassmann, T., Petrovic, N., et al., 2007. Myogenic gene expression signature establishes that brown and white adipocytes originate from distinct cell lineages. Proceedings of the National Academy of Sciences of the United States of America 104(11): 4401–4406. https://doi.org/10.1073/pnas.0610615104.

[39] Kazak, L., Chouchani, E.T., Jedrychowski, M.P., Gygi, S.P., Bruce, M., Kazak, L., et al., 2015. A creatine-driven substrate cycle enhances energy expenditure and thermogenesis in beige fat article a creatine-driven substrate cycle enhances energy expenditure and thermogenesis in beige fat. Cell 163(3):643–655. https://doi.org/10.1016/j.cell.2015.09.035.

[40] Müller, S., Balaz, M., Stefanicka, P., Varga, L., Amri, E.-Z., Ukropec, J., et al., 2016. Proteomic analysis of human Brown adipose tissue reveals utilization of coupled and uncoupled energy expenditure pathways. Scientific Reports 6(May):30030. https://doi.org/10.1038/srep30030.

[41] Shinoda, K., Luijten, I.H.N., Hasegawa, Y., Hong, H., Sonne, S.B., Kim, M., et al., 2015. Genetic and functional characterization of clonally derived adult human brown adipocytes. Nature Medicine 21(4):389–394. https://doi.org/10.1038/nm.3819.

[42] Bradshaw, A.D., Graves, D.C., Motamed, K., Sage, E.H., 2003. SPARC-null mice exhibit increased adiposity without significant differences in overall body weight. Proceedings of the National Academy of Sciences of the United States of America 100(10):6045–6050. https://doi.org/10.1073/pnas.1030790100.

[43] Yan, J., Burman, A., Nichols, C., Alila, L., Showe, L.C., Showe, M.K., et al., 2006. Detection of differential gene expression in brown adipose tissue of hibernating arctic ground squirrels with mouse microarrays. p. 346–53. https://doi.org/10.1152/physiolgenomics.00260.2005.

[44] Larsen, T.J., Jespersen, N.Z., Scheele, C., 2018. Adipogenesis in primary cell culture, vol. 7. Handbook of Experimental Pharmacology.

[45] Becker, A.S., Nagel, H.W., Wolfrum, C., Burger, I.A., 2016. Anatomical grading for metabolic activity of Brown adipose tissue. PLoS One 11(2):e0149458. https://doi.org/10.1371/journal.pone.0149458.

[46] Leitner, B.P., Huang, S., Brychta, R.J., Duckworth, C.J., Baskin, A.S., McGehee, S., et al., 2017. Mapping of human brown adipose tissue in lean and obese young men. Proceedings of the National Academy of Sciences of the United States of America 114(32):6–11. https://doi.org/10.1073/pnas.1705287114.

[47] Petrovic, N., Walden, T.B., Shabalina, I.G., Timmons, J.A., Cannon, B., Nedergaard, J., 2010. Chronic peroxisome proliferator-activated receptor gamma (PPARG) activation of epididymally derived white adipocyte cultures reveals a population of thermogenically competent, UCP1-containing adipocytes molecularly distinct from classic brown adipocytes. Journal of Biological Chemistry 285(10):7153–7164. https://doi.org/10.1074/jbc.M109.053942.

[48] Seale, P., Conroe, H.M., Estall, J., Kajimura, S., Frontini, A., Ishibashi, J., et al., 2011. Prdm16 determines the thermogenic program of subcutaneous white adipose tissue in mice. Journal of Clinical Investigation 121(1):96–105. https://doi.org/10.1172/JCI44271.

[49] Wang, Q.A., Tao, C., Gupta, R.K., Scherer, P.E., 2013. Tracking adipogenesis during white adipose tissue development, expansion and regeneration. Nature Medicine 19(10):1338–1344. https://doi.org/10.1038/nm.3324.

[50] Lee, Y.H., Petkova, A.P., Mottillo, E.P., Granneman, J.G., 2012. In vivo identification of bipotential adipocyte progenitors recruited by β3-adrenoceptor

activation and high-fat feeding. Cell Metabolism 15(4):480–491. https://doi.org/10.1016/j.cmet.2012.03.009.

[51] Rosenwald, M., Perdikari, A., Rülicke, T., Wolfrum, C., 2013. Bi-directional interconversion of brite and white adipocytes. Nature Cell Biology 15:659.

[52] Scheele, C., Nielsen, S., 2017. Metabolic regulation and the anti-obesity perspectives of human brown fat. Redox Biology 12(Aug):770–775. https://doi.org/10.1016/j.redox.2017.04.011.

[53] Søndergaard, E., Gormsen, L.C., Christensen, M.H., Pedersen, S.B., Christiansen, P., Nielsen, S., et al., 2015. Chronic adrenergic stimulation induces brown adipose tissue differentiation in visceral adipose tissue. Diabetic Medicine 32(2):e4–e8. https://doi.org/10.1111/dme.12595.

[54] Bar-Shalom, R., Gaitini, D., Keidar, Z., Israel, O., 2004. Non-malignant FDG uptake in infradiaphragmatic adipose tissue: a new site of physiological tracer biodistribution characterised by PET/CT. European Journal of Nuclear Medicine and Molecular Imaging 31(8):1105–1113. https://doi.org/10.1016/S1040-1741(08)70025-3.

[55] Yeung, H.W.D., Grewal, R.K., Gonen, M., Schöder, H., Larson, S.M., 2003. Patterns of (18)F-FDG uptake in adipose tissue and muscle: a potential source of false-positives for PET. Journal of Nuclear Medicine – Official Publication Society of Nuclear Medicine 44(11):1789–1796.

[56] Atherton, D.S., Deep, N.L., Mendelsohn, F.O., 2012. Micro-anatomy of the renal sympathetic nervous system: a human postmortem histologic study. Clinical Anatomy 25(5):628–633.

FURTHER READING

[27] Littell, Ramon C., Milliken, George A., Stroup, W.W., Wolfinger, Russell D., O.S., 2006. SAS for mixed models, 2nd ed. Cary, NC: SAS Institute Inc.

